Perimeter traffic control strategy based on macroscopic fundamental diagrams

Xu Jianmin　　Yan Xiaowen　　Ma Yingying　　Jing Binbin

(School of Civil Engineering and Transportation, South China University of Technology, Guangzhou 510640, China)

Abstract: A perimeter traffic signal control strategy is proposed based on the macroscopic fundamental diagram theory (MFD) to solve the signal control problem in oversaturated states. First, the MFD of a specific regional network can be derived using VISSIM simulation software. Secondly, the maximum number of cumulative vehicles that the network can accommodate is determined based on the MFD. Then, through monitoring the influx flow, the number of vehicles existing in and exiting from the network, a perimeter traffic control model is proposed to optimize the signal timing of the boundary intersections. Finally, a virtual network simulation model is established and three different kinds of traffic demand are loaded into the network. Simulation results show that after the strategy implementation, the number of vehicles accumulating in the network can be kept near the optimal value, while the number of both entering and exiting vehicles increases significantly and the road network can be maintained at a large capacity. Simultaneously, the queue length at the approach of the border intersections is reasonably controlled and vehicles entering and exiting the network can maintain a more efficient and stable speed. The network performance indices such as the average traffic delay and average number of stops can be improved to a certain degree, thus verifying the effectiveness and feasibility of the perimeter control strategy.

Key words: macroscopic fundamental diagram; perimeter control; green duration optimization; microscopic simulation

DOI: 10. 3969/j. issn. 1003 − 7985. 2017. 04. 018

Problems related to traffic congestion in large and medium-sized cities have become increasingly prominent, particularly in centralized cities. Although traffic management agencies have proposed a variety of efficient control strategies to ease congestion, the actual impact of

these countermeasures has not been as effective as expected. The effectiveness of traffic control strategies cannot be adequately evaluated without building reasonable traffic forecasting models at the macroscopic level. Macroscopic modeling of the urban gridlock was first proposed by Daganzo[1], and a well-defined macroscopic fundamental diagram (MFD) of urban traffic, the relationship between average network flow and vehicle accumulation in the road network, was later proposed by Geroliminis et al[2]. Researchers argued that the MFD can reflect the relationship among road network parameters, such as output flow and number of vehicles in the region[3], total amount of traffic flow, average density of the road network[4], total vehicle mileage, and gross vehicle running time[5-6]. Meanwhile, researchers proposed evidence of the existence of MFD using both the field data[7-10] and traffic simulation[9-12], and explored the applications of the MFD in network management and control. In terms of applications for different control objectives, the control objectives can be divided into maximal total outflow of the road network[12-16], optimal cumulative number of vehicles in the network[17], and the network density maintaining at an appropriate level[18]. It can also be divided into optimal perimeter control[13-15], bang-bang control[17], model predictive control[16], area metering control[18], and feedback gate control[19], based on different control methods. Another related study[12] on road network boundary control proposed a network layer control strategy based on traffic sub-zones, but the research lacked a clear description of the connection between the network layer and the sub area layer. Although previous studies have proposed the idea of implementing border control based on the MFD[20], the effective control strategy was lacking. While the border control strategy proposed in Refs. [13 − 15, 21] is far more complex, Ref. [16] required a rather high accuracy of the prediction model, which is difficult to maintain under realistic conditions and it also lacks consideration of the network capacity.

Therefore, on the basis of previous studies, a novel border control method for near-saturated road networks is proposed. In light of the near-saturated network, considering the premise of the carrying capacity of the entire network, an effective signal optimization scheme at border intersections is proposed. The macroscopic properties

of the MFD are utilized to ensure that the total number of vehicles in the network remains reasonably practicable at both the macroscopic and microscopic levels. This method is far more operable and it is more suitable for realistic road network conditions.

1 MFD Theory

It is feasible to derive a macroscopic fundamental diagram from a simulation experiment or from traffic data collected directly at a field site. The MFD obtained by these two methods can be used as the basis for the adjustment of the signal timing scheme. For a specific network experiment, given different origin-destination demand, traffic demand is allocated to determine the inflow, the road traffic, the crossing traffic, and turning ratio of the border network with the aid of transportation planning software TransCAD. Then, signal timing plans are set up using microscopic simulation software VISSIM. To derive the MFD of a network, the linked traffic variables such as flow and density are needed. There should be as many measured links as possible, thus the macroscopic fundamental diagram can be derived to reflect the network traffic situation correctly. The data at the network level are easily generated by averaging the linked data, and the weighted average flow and density were recommended for use by Daganzo[1]. The relationship between the related parameters is as follows:

$$
\left.
\begin{aligned}
N &= \sum_i k_i l_i \\
q^w &= \sum_i q_i l_i \Big/ \sum_i l_i \\
k^w &= \sum_i k_i l_i \Big/ \sum_i l_i
\end{aligned}
\right\}
\tag{1}
$$

where N represents the number of accumulating vehicles in the network; k_i, q_i and l_i denote density, traffic flow, and length of road i, respectively; q^w and k^w represent weighted average flow and density. The relationship between the weighted average flow and the number of accumulated vehicles in the road network can be established by combining the use of TransCAD and VISSIM software. By fitting the simulation data, the result of the fitting function relationship can be derived, which is a macroscopic fundamental diagram.

2 Perimeter Traffic Control Strategy

2.1 Hypothesis

The control model must be constructed with the following assumptions: 1) The ratios of the traffic flow among right-turn, left-turn and through directions at each entry link are all constants in the analysis period; 2) The four-phase signal control scheme, i. e., the through phase for east-west direction, left turn phase for east-west direction, through phase for south-north direction, left turn

phase for south-north direction, is used by each intersection; 3) All the entry links about the boundaries of the control area are long enough to accommodate the vehicles held outside the network, regardless of the signal timing of the upstream intersection; 4) Phase transition time is ignored.

2.2 Control strategy

The basic idea of perimeter signal control based on the MFD is to monitor influx flow, total vehicles in the network, and outflows from the network. By restricting the amount of influx flow proportionally, the accumulating vehicles in the network can be maintained within a reasonable and practicable range. The core concept of establishing the control model based on MFD is to first determine the number of critical cumulative vehicles that the control area can accommodate according to the MFD. Then, based on the macroscopic state evolution equation, the allowable number of entering vehicles in the next control period can be calculated. Then, flow limits are imposed on boundary intersections. The boundary signal control model proposed in this paper is not for all the boundary intersections, but for the intersection whose total flow ratio is greater than 0.9. It means that the traffic demand exceeds the capacity and there is not enough green time to release the vehicles arriving from all directions. Some vehicles will have to be queued at the entrance for several cycles to pass through, which may most likely lead to queuing overflow. Considering the restrictions of queue length at the entry link and the rest of the capacity of downstream sections at the approach of the border intersections, the specific vehicles that can be allowed to enter is determined. Finally, the appropriate green time is assigned to the corresponding import phase according to the restricted entering vehicles.

The evolution equation of the macroscopic state of the road network in discrete form is as follows:

$$
N(a+1) = N(a) + I(a) - O(a) \tag{2}
$$

where $N(a+1)$ and $N(a)$ represent the number of accumulating vehicles at the $(a+1)$-th and the a-th sampling interval, respectively; $I(a)$ and $O(a)$ represent the influx flow and outflow for road network at the a-th sampling interval, respectively, veh.

The influx and output flow are closely related to the signal cycle, saturation flow rate and green duration ratio of the border entrance phase, and thus, the input and output flow meet the following equation:

$$
\left.
\begin{aligned}
I(a) &= \sum_{j \in J} \sum_{h \in H} C_j(a) g_{jh}(a) s \\
O(a) &= \sum_{j \in J} \sum_{h \in H} C_j(a) g'_{jh}(a) s
\end{aligned}
\right\}
\tag{3}
$$

The following equation can be derived from iteration:

$$N(a) = N(0) + \sum_{p=0}^{a-1} \sum_{j \in J} \sum_{h \in H} C_j(p)s \cdot$$
$$[g_{jh}(p) - g'_{jh}(p)] \tag{4}$$

where $N(0)$ denotes the number of vehicles in the road network at the initial time; C_j is the intersection signal cycle, s; s is the saturation flow rate, veh/s; g_{jh} and g'_{jh} represent the green duration ratio of the h-th import and the exit phase of the j-th intersection, respectively; J and H represent the set of the intersections and the imports of intersections, respectively.

The control objective of the boundary strategy based on MFD is to maintain the cumulative number of vehicles near the optimal value by optimizing the cycle and green duration ratio of the border intersection. The boundary control model is established and the objective function is

$$\min Z = \frac{1}{2} \sum_{a=1}^{M} \Big[N(0) + \sum_{p=0}^{a-1} \sum_{j \in J} \sum_{h \in H} C_j(p)s \cdot$$
$$[g_{jh}(p) - g'_{jh}(p)] - N_c \Big]^2 \tag{5}$$

s. t.

$$Q^{in} \leqslant N_c + O(a-1) - N(a-1) \tag{6a}$$

$$\sum_h \frac{q_{jh}}{s_{jh}} \geqslant 0.9 \tag{6b}$$

$$Q_j^{in} = C_j s \sum_{h \in H} g_{jh}(a) \tag{6c}$$

$$Q_j^{in} \leqslant Q^{in} \frac{\sum_h L_{qb,jh}/(L_i k_{jam,i} n_i)}{\sum_j \sum_h L_{qb,jh}/(L_i k_{jam,i} n_i)} \tag{6d}$$

$$Q_j^{in} \leqslant Q^{in} \frac{(L_f - L_{q,f}) k_{jam,f} n_f}{Q_j^{in}} \tag{6e}$$

$$g_{min} \leqslant C_j(a) g_{jh}(a) \leqslant g_{max} \tag{6f}$$
$$g_{min} \leqslant C_j(a) g'_{jh}(a) \leqslant g_{max} \tag{6g}$$
$$C_{min} \leqslant C_j(a) \leqslant C_{max} \tag{6h}$$

where N_c represents the optimal cumulative number of vehicles, veh; M is the number of control steps; Q^{in} denotes the restricted allowed influx flow, veh; q_{jh} and s_{jh} represent the actual flow and saturated flow at the approach of intersection, respectively, veh/s; Q_j^{in} denotes the restricted allowed influx flow of the j-th intersection, veh; $L_{qb,jh}$ represents the number of queuing vehicles at the approach of the border intersection, veh; L is the road length, m, k_{jam} is the blocking density of each link, veh/m; n is the number of lane s; i and f represent the road at the approach of the border intersection and the road downstream of the approach of the border intersection, respectively; $L_{q,f}$ represents the maximal queuing length downstream of the approach of the border intersection, m; g_{min}, g_{max} and C_{min}, C_{max} represent the minimum and maximum green duration and cycle length, respectively.

Constraint (6a) shows the constrained total amount of the volume that allows access to the control area and is derived from the vehicle conservation equation. Constraint (6b) shows the critical intersection constraint that must implement the influx flow control, which satisfies the condition that the total flow ratio of the intersection exceeds 0.9. Constraints (6c) to (6e) show the allowable influx constraint of the entrance phase of the border intersection considering the approach queue length and the remaining capacity constraint of the downstream section. Constraints (6f) to (6h) show the maximum and minimum constraints that green duration and cycle length should meet.

2.3　Model solving

The optimization model established in this paper determined the allowable constrained influx flow considering the load capacity of the entire network. Then, focusing on border intersections, the green duration and cycle length are optimized considering the entrance queue length and the remaining capacity constraints of the downstream section. The control model is a nonlinear programming model and its decision variables are cycle length and green duration. The model involves both the variables and nonlinear constraints. It is difficult to determine the global optimal solution using the traditional nonlinear programming method. However, the genetic algorithm has a significant effect on solving the highly complex search space problem. Therefore, the genetic algorithm is used to solve the model. The solving process is as follows:

Step 1 Set the value of crossover probability p_c and mutation probability p_m of the genetic algorithm, respectively, to be 0.6 and 0.02. The total number of individuals per generation G and the maximum number of iterations Q values are 40 and 100, respectively. Real number encoding is used and the code is $(C_1, \cdots, C_j, g_{11}, \cdots, g_{jh})$, in which the minimum and maximum values of green duration and cycle length are, respectively, 10, 70 and 60, 180.

Step 2 (Initialization of the population) Generate p_1 individuals randomly in the search domain and adjust the points to meet the constraints to establish the initial population pop(0) and set $b = 0$.

Step 3 (Fitness function) Calculate the fitness function value of each point in pop(b) and find the point with the minimum function and minimum fitness value. The fitness function is $f = 1/Z$, in which Z is the objective function value.

Step 4 (Crossover operator) For each individual $p \in$ pop(b), p_c is the crossover probability. First, select one value of r from 0 to 1 randomly, if r is smaller than or equal to p_c, then the crossover operation is performed on the individual to determine cross offspring p_0, and let O_1 signify a collection of all cross-generation.

Step 5 (Mutation operator) For each individual $p \in$ pop(b), p_m is the mutation probability. First, select one value of r from 0 to 1 randomly, if r is smaller or

equal to p_m, then the mutation operation is performed on the individual to determine cross offspring p'_0, and let O_2 signify a collection of all mutation-generation.

Step 6(Selection)   Let $O = O_1 \cup O_2$. Select n_1 individuals with the smallest fitness value, in which n_1 is smaller than p_1 and select $p_1 - n_1$ individuals from the remaining to form the next generation pop($b + 1$).

Step 7 (Judgment)   If the iteration times reach the maximum, calculation is stopped and the optimal solution is produced. Otherwise, set $b = b + 1$ and go to Step 3.

3   Analysis of Simulation Test

3.1   Road network description and simulation parameter calibration

To demonstrate the efficiency of the proposed approach, a hypothetical simulation network of 12 entrances and 12 exits is designed, as shown in Fig. 1. The number of bi-directional road lanes is 6 and the length of each section is assumed to be 400 m. The OD demand and signal timing plan of all the intersection are set in the simulation model and detectors are set up at the entrance and exit of the border intersections. The duration of a complete simulation is 3 600 s and the first 5 min is assumed to be the initialization process. Six simulation experiments were carried out by changing the random seed parameter in VISSIM, and statistical data was recorded every 5 min, including the influx flow, outflow, traffic flow on every road, and the number of moving vehicles in the road network.
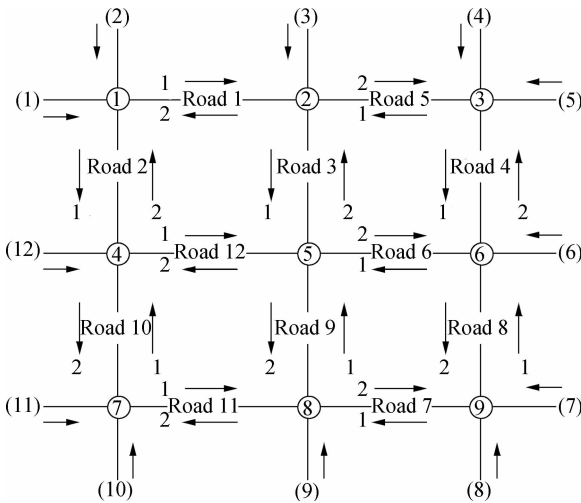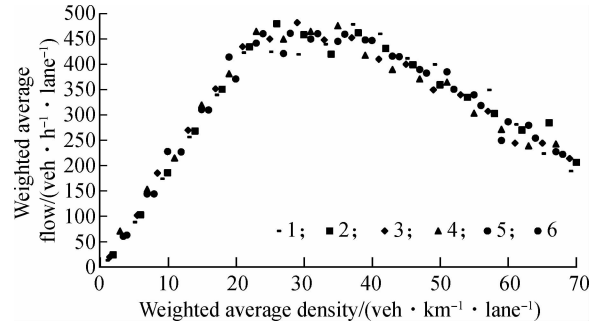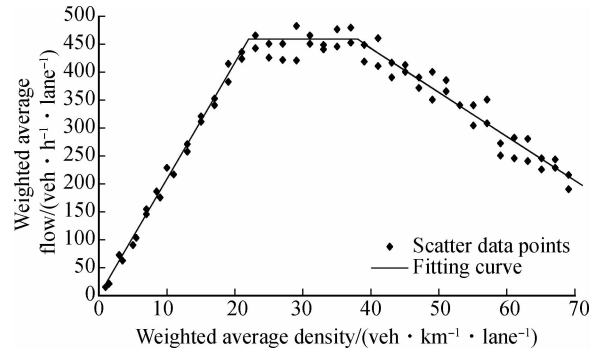

Fig. 1   Hypothetic network

3.2   Construction of MFD in the test area

The OD demand loaded in the simulation model is increased by 30% successively on the basis of the off-peak hour OD demand. The study simulated the entire process of traffic flow evolving from off-peak hour to peak hour and finally to oversaturation. The weighted average density and weighted average flow are taken as horizontal and vertical coordinates, respectively, and the MFD data fitting curve is derived from processing six sets of simulation data, as shown in Fig. 2(a), for which the legend of different shapes represents a one-time complete simulation result.

(a)

(b)

Fig. 2   Curve trend of MFD. (a) MFD data fitting curve of road network; (b) Similar trapezoidal diagram of MFD

From the scatter plot shown in Fig. 2(a), with the increase of the weighted average density in the network, the weighted average flow increases first, then maintains a high level, and gradually decreases at the end. Therefore, the MFD curve can be divided into three parts: ascent stage, continuous segment, and descent section. The fast clustering method (K-means) can be used to group these data and distinguish between three intervals. Concerning the data characteristics in each curve, the least square method can be used to fit the curve of the scatter plot in both the ascent and continuous sections, while the falling section curve can be fitted by using the average data point method. Hence, a complete macroscopic fundamental diagram can be derived, which is similar to a trapezoid, as shown in Fig. 2 (b). The expression of the MFD fitting curve is as follows:

$$y(x) = \min\{y_1(x), y_2(x), y_3(x)\} \qquad (7)$$

The expression of the piecewise function is

$$\left.\begin{array}{ll} y_1(x) = 20.86x & 0 \leqslant x \leqslant 22 \\ y_2(x) = 459 & 22 < x \leqslant 38 \\ y_3(x) = -7.9x + 759.2 & 38 < x \leqslant 94 \end{array}\right\} \qquad (8)$$

where x represents the weighted average density and $y(x)$ denotes the weighted average flow. The correlation coefficients are, respectively, 0.98, 0.92, 0.94, which is close to 1 and the result can achieve a high degree of fitting, meeting the requirement of the follow-up quantitative calculation.

3.3 Simulation of perimeter traffic control strategy based on MFD

The critical threshold of the accumulating flow in the road network can be determined according to the MFD fitting curve. Using the Matlab genetic algorithm toolbox to compile the entire control program, the algorithm can output the optimal signal cycle and green duration for the border intersection. Relevant performance indices related to the whole network, road sections and the approach are analyzed comparatively before and after the strategy implementation. When the saturation of the intersection is between 0.8 and 0.9, it is defined as the near-saturated state. When the saturation of the intersection is greater than 0.9, it is defined as the super-saturated state. To verify the effectiveness of the boundary control method, the simulation tests were carried out under three different levels of traffic demand: medium, high and super high, respectively, which corresponds to an unsaturated, near-saturated and super-saturated state, respectively. Different traffic demand values for the border entrances are shown in Tab. 1.

Tab. 1 Traffic demand values for border entrances   km/h

Level of traffic demand	Entrance											
	1	2	3	4	5	6	7	8	9	10	11	12
Medium	1 056	750	743	944	1 040	1 063	1 019	846	928	863	1 085	1 138
High	1 373	975	966	1 227	1 352	1 382	1 325	1 100	1 206	1 122	1 411	1 479
Super high	1 785	1 268	1 256	1 595	1 758	1 796	1 722	1 430	1 568	1 458	1 834	1 923

The legends M, H and SH, respectively, denote medium, high, super high traffic demand, as shown in Fig. 3 (a). Comparatively analyzing the results under different traffic demands, the curves of the number of vehicles entering and exiting the network varying with time per unit interval all show a stable rate first, then decrease sharply, and finally keep stable. However, the difference between the stability rates under different levels of demand is sizable. The entering flow stabilizes at approximately 150, 185 and 170 veh/h, respectively, under the conditions of super high, high, and medium traffic demand while the exit flow stabilizes at 40, 150 and 150 veh/h, respectively. The exiting flow shows no significant difference between medium and high demand. While in super high demand, the gap is quite obvious and the exiting flow drops to 40 veh/h, meaning that most vehicles are unable to
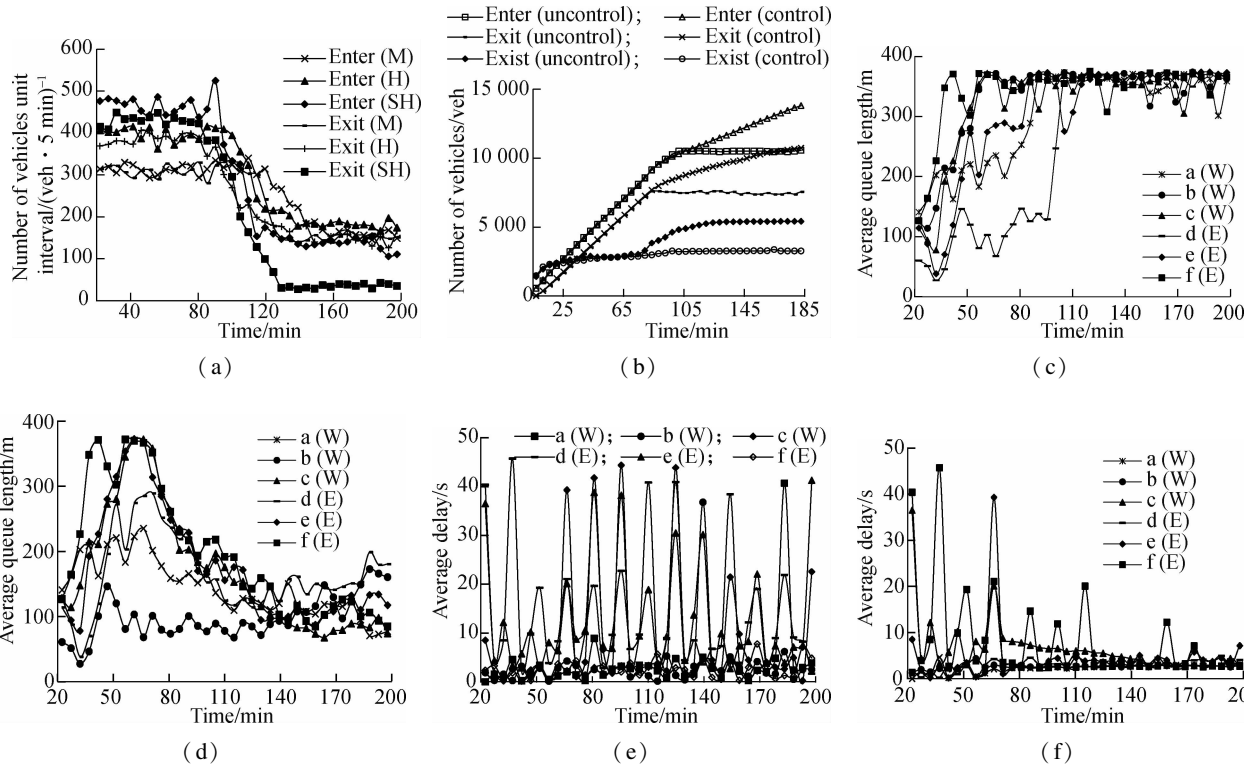

Fig. 3 Change of traffic flow and comparison of queue length and average delay before and after strategy implementation. (a) Number of entering and exiting vehicles per unit interval under different traffic demands; (b) Number of entering, exiting and existing vehicles under super high demand; (c) Queue length (uncontrol); (d) Queue length (control); (e) Average delay (uncontrol); (f) Average delay (control)

leave the network. On the other side, the entering flow under super high demand is lower than that under high demand. Therefore, there is no need to implement border control under the medium traffic demand conditions when the cumulative number of vehicles in the network is less than the capacity threshold and the traffic enters and exits relatively smoothly allowing the network capacity to maintain a certain level. While under the conditions of high and super high demand, with the simulation running at 4 500 s, the number of vehicles entering and exiting sharply decreases and the road network is likely to enter saturation mode. Thus, it is quite necessary to limit the influx flow at boundary intersections at this time.

The number of accumulating entering, accumulating exiting, and existing vehicles for the network varying with time is shown in Fig. 3(b) under the condition of super high demand. The legends control and uncontrol, respectively, indicate that the signal timing is optimized with the boundary control model and the original pre-timed signal plan stays unchanged. For no perimeter control, with the increase of accumulating vehicles entering the network, the cumulative number of vehicles gradually increases to the maximum, which stays at approximately 5 042 under super high demand. After a certain period, the network is nearly saturated and the number of vehicles accumulating to enter and exit reaches the maximum and remains unchanged, which is nearly 9 814 and 6 891 under super high demand. That is, vehicles are unable to enter or exit the network

and the network tends to be in deadlock mode. When implementing border control, the cumulative number of vehicles continues to fluctuate within the vicinity of the optimal value 3 062, and the number of accumulating entering and exiting vehicles increases continuously at a certain rate until the traffic capacity reaches the maximum.

In the current experiment, east-west is the main direction of the network. When the simulation runs 4 500 s, the border control strategy is adopted. The travel speed curve and average queue length of 12 sections of the east-west boundary, and the average delay of 6 intersection entrances varying with time before and after the control implementation are shown in Figs. 3(c) to (f) and Fig. 4. The legends a(W) and d(E) represent the west entrance of boundary intersection a and east entrance of boundary intersection d. a,b,c,d,e,f, respectively, represent six boundary intersections of the road network. And W and E, respectively, represent the west and east entrance of the boundary intersection. E and I, respectively, represent the exit and import sections in Fig. 4(e), while D and Q, respectively, represent average delay and average queue length for all entrances in Fig. 4(f).

As shown in Fig. 3 and Fig. 4, when the simulation runs 4 500 s, the queue length of the border entrance is close to the maximum and the queuing overflow phenomenon occurs in many approaches. The speed of vehicles entering decreases sharply and approach delay increases greatly.
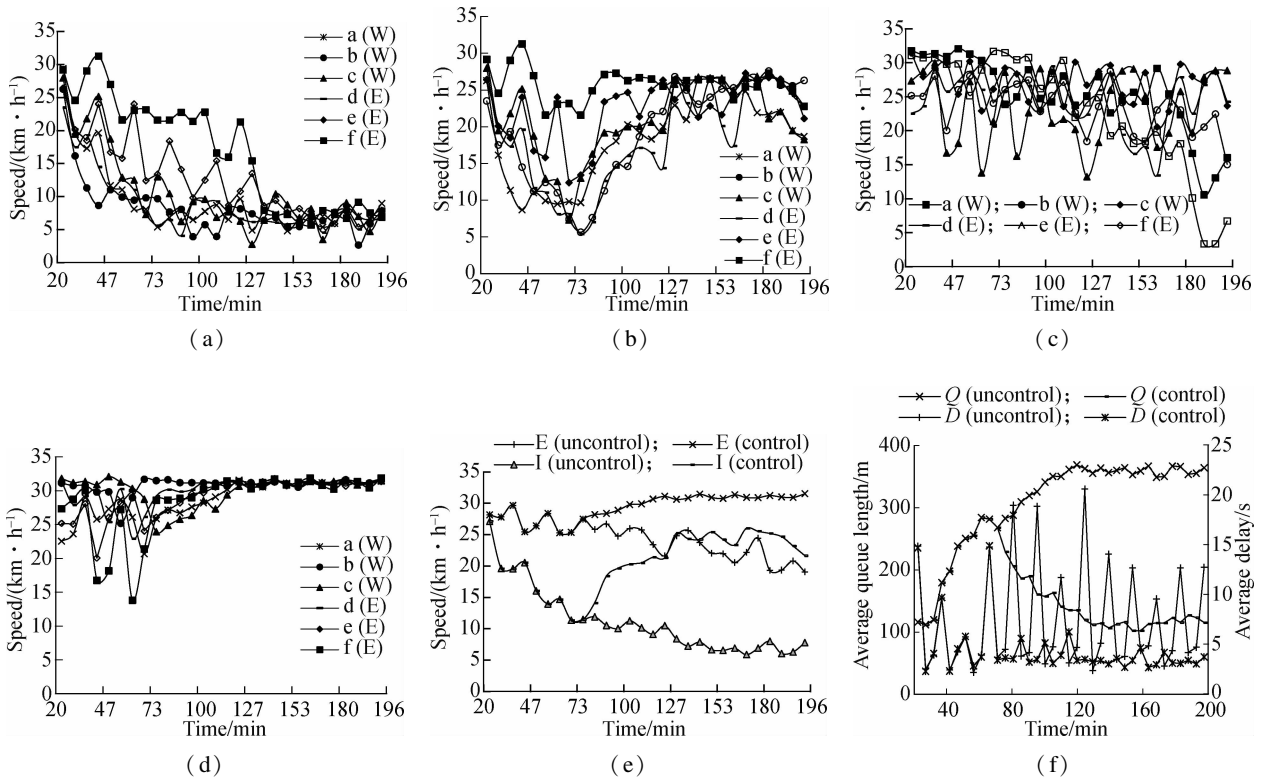

Fig. 4 Comparison of performance indices varying with time before and after the strategy implementation. (a) Entrance section (uncontrol); (b) Entrance section (control); (c) Exit section (uncontrol); (d) Exit section (control); (e) Road speed; (f) Queue length and average delay

Comparing Figs. 3(c) and (d), after the strategy implementation, the queuing length of each approach is improved to some extent and the maximum queue length is limited to about 160 m, which greatly avoids the overflow phenomenon. In addition, vehicle delay is greatly reduced, as shown in Figs. 3(e) and (f). In contrast with Figs. 4(a) and (b), the border entrance queue length is long and the speed of vehicles entering is low under the original signal timing. However, after the strategy implementation, the speed at the border approach increases from 8 to 25 km/h. Figs. 4(c) and (d) show that the speed of the export section also increases modestly and can be stabilized at nearly 30 km/h, which can essentially achieve the goal of vehicles entering slowly and exiting rapidly. Figs. 4(e) and (f) clearly demonstrate the space for speed improvement and effects for queue length, while vehicle delay decreases before and after control.

The three-dimensional map is used to show the status change of the network before and after control implementation in both the high and super high flow demand. The time is represented on the Z axis, while the number of vehicles in and leaving the network are represented on the X and Y axes, respectively. The number of vehicles with the change of time is plotted in Fig. 5.

Comparative analyses of Figs. 5(a) and (c) show that in the absence of border control, the higher the traffic demand, the sooner the road network achieves saturation and the lower the ultimate departure capability of the network is. In comparison with Figs. 5(b) and (d), after implementing control, the number of vehicles in the network can maintain at about 3 000 in the near-saturated state and the output capacity of the road network can be maintained at a higher stationary value. While in a super-saturated state, the cumulative number of vehicles first maintains at around 3 000, but with the evolution of time, the cumulative number of vehicles gradually reduces to about 2 000, and the number of vehicles leaving the road network cannot maintain at a high and stable value. The effect of boundary control strategy is more significant under the high traffic demand conditions. The border control strategy may temporarily slow down the traffic pressure to maintain a certain output capacity under super high demand. However, if the heavy load demand persists, the output capacity will be affected to a certain degree. Therefore, this model is more suitable for near-saturated conditions with a moderate flow. In addition, with boundary flow control, it is necessary to implement a reasonable traffic management strategy for oversaturated conditions with excessive traffic demand. The comparison of performance indices of the network before and after the strategy implementation across the entire simulation time is shown in Tab. 2.

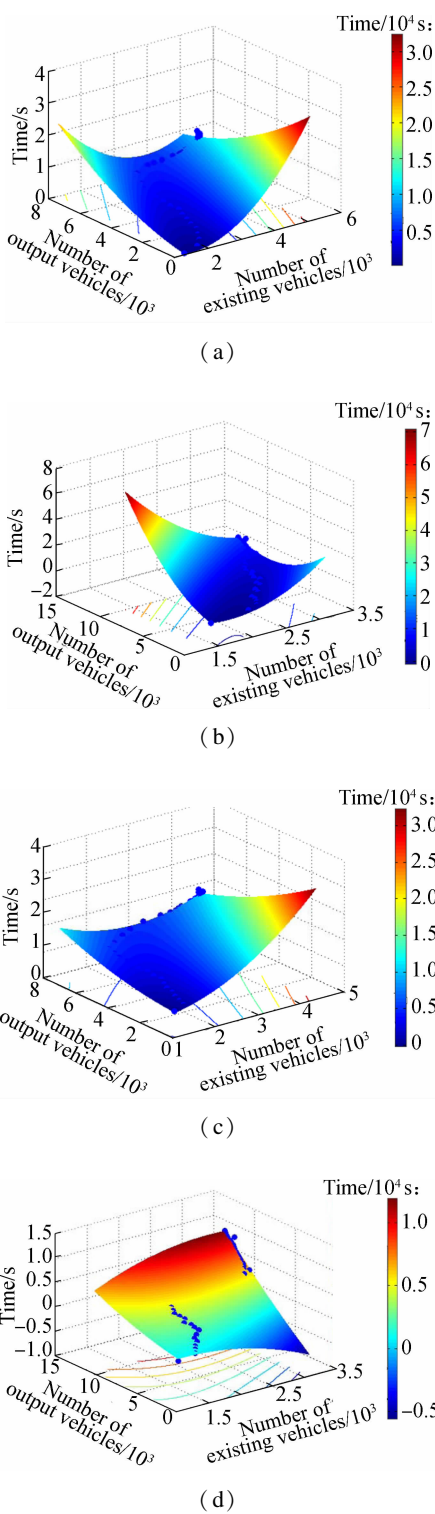Tab. 2 shows the comparison of simulation results before

(a)

(b)

(c)

(d)

Fig. 5 Entering and exiting flow and cumulative vehicular numbers with and without road network control in the congestion area. (a) Under super high demand(uncontrol); (b) Under super high demand(control); (c) Under high demand(uncontrol); (d) Under high demand(control)

and after control implementation. The following improvement can be obtained by calculation. The average delay is reduced by 26. 23% and 15. 8%, respectively, and the average stops is reduced by 22. 9% and 22. 2%, respectively, under high and super high demand. Although the

border control strategy limits a certain number of vehicles entering the network, the total throughput is improved. The number of entering vehicles increased by 33. 8% and 23. 8%, respectively, and the number of output vehicles increased by 31. 5% and 29. 6%, respectively, under high and super high demand. The output capacity of the network has been greatly improved.

Tab. 2 Comparison of performance indices of the network

Traffic demand	Scheme	Average delay/s	Average stops	Number of entering vehicles	Number of exiting vehicles
High	Uncontrol	9. 76	5. 29	8 010	7 058
	Control	7. 2	4. 08	12 099	10 305
Super high	Uncontrol	15. 2	9. 72	9 814	6 891
	Control	12. 8	7. 56	12 882	9 792

4 Conclusion

This study introduces a new regional perimeter control strategy based on the macroscopic fundamental diagram (MFD) theory. The optimal cumulative traffic carrying capacity of a specific road network, therefore, is obtained through simulation, and an optimization control strategy considering carrying capacity comprehensively in the network and intersection level is designed. Through cycle length and green duration optimization of the border intersections, the inflow from perimeter intersections is controlled reasonably, thus maintaining a near saturation state at every intersection in the network. The simulation result indicates that the strategy can control the queue length effectively and ensure that the network maintains a large output capacity.

The boundary optimization strategy is easy to implement by optimizing the signal control scheme of the intersection under high traffic demand conditions. Queue length can be controlled reasonably to ensure the capacity of the road network, which is exceptionally efficient for the near saturated traffic state. One of the disadvantages is that this model merely optimizes the signal scheme of boundary intersections, but it fails to consider internal intersections. In addition, the model assumes that the entrance section is long enough and artificially eliminates the possibility of upstream queuing overflow out of the control area, which may appear with boundary control implementation. In fact, the queuing overflow phenomenon of the upstream may exist in reality. The future work is, therefore, to design a boundary control strategy that considers the capacity constraints of the upstream sections of border intersections and delineates the control boundaries rationally.

References

[1] Daganzo C F. Urban gridlock: Macroscopic modeling and mitigation approaches [J]. *Transportation Research Part B: Methodological*, 2007, **41**(1): 49 − 62. DOI: 10. 1016/j. trb. 2006. 03. 001.

[2] Geroliminis N, Sun J. Properties of a well-defined macroscopic fundamental diagram for urban traffic [J]. *Transportation Research Part B: Methodological*, 2011, **45**(3): 605 − 617. DOI: 10. 1016/j. trb. 2010. 11. 004.

[3] Cassidy M J, Jang K, Daganzo C F. Macroscopic fundamental diagrams for freeway networks theory and observation [J]. *Transportation Research Record*, 2011, **2260**: 8 − 15. DOI: 10. 3141/2260-02.

[4] Xu F F, He Z C, Sha Z R. Impacts of traffic management measures on urban network microscopic fundamental diagram [J]. *Journal of Transportation Systems Engineering and Information Technology*, 2013 (2): 185 − 190.

[5] Gonzales E J, Chavis C, Li Y, et al. Multimodal transport modeling for Nairobi, Kenya: Insights and recommendations with an evidence-based model, UCB-ITS-VWP-2009-5 [R]. Berkeley, USA: UC Berkeley Center for Future Urban Transport, 2009.

[6] Du Y M, Wu J P, Jia Y H, et al. MFD-based regional traffic volume dynamic control [J]. *Journal of Transportation Systems Engineering and Information Technology*, 2014, **35**(3): 162 − 167.

[7] Buisson C, Ladier C. Exploring the impact of homogeneity of traffic measurements on the existence of macroscopic fundamental diagrams [J]. *Transportation Research Record*, 2009, **2124**: 127 − 136. DOI: 10. 3141/2124-12.

[8] He Z, He S, Guan W. A figure-eight hysteresis pattern in macroscopic fundamental diagrams and its microscopic causes [J]. *Transportation Letters: The International Journal of Transportation Research*, 2015, **7**(3): 133 − 142. DOI: 10. 1179/1942787514y. 0000000041.

[9] Xie X, Chiabaut N, Leclercq L. Macroscopic fundamental diagram for urban streets and mixed traffic cross comparison of estimation methods [J]. *Transportation Research Record*, 2013, **2390**: 1 − 10. DOI: 10. 3141/2390-01.

[10] Ji Y, Daamen W, Hoogendoorn-Lanser S, et al. Investigating the shape of the macroscopic fundamental diagram using simulation data [J]. *Transportation Research Record*, 2010, **2161**: 40 − 48. DOI: 10. 3141/2161-05.

[11] Stamos I, Salanova Grau J M, Mitsakis E, et al. Macroscopic fundamental diagrams: Simulation findings for the ssaloniki's road network [J]. *International Journal for Traffic and Transport Engineering*, 2015, **5**(3): 225 − 237. DOI: 10. 7708/ijtte. 2015. 5(3). 01.

[12] Ma Y Y. Study of sub-network-oriented traffic signal control strategy [D]. Shanghai: College of Transportation Engineering, Tongji University, 2010. (in Chinese)

[13] Aboudolas K, Geroliminis N. Perimeter flow control in heterogeneous networks [C]//13th Swiss Transport Research Conference. Ascona, Switzerland, 2013: 1055 − 1081.

[14] Aboudolas K, Geroliminis N. Perimeter and boundary flow control in multi-reservoir heterogeneous networks [J]. *Transportation Research Part B: Methodological*, 2013, **55**: 265 − 281. DOI: 10. 1016/j. trb. 2013. 07. 003.

[15] Aboudolas K, Geroliminis N. Feedback perimeter control

for multi-region large-scale congested networks ［C］// 2013 *European Control Conference*. Zurich, Switzerland, 2013:106 － 114.

［16］Haddad J, Ramezani M, Geroliminis N. Model predictive perimeter control for urban areas with macroscopic fundamental diagrams ［C］//*American Control Conference*. Montreal, QC, Canada, 2012:5757 － 5762.

［17］Zhang Y, Bai Y, Yang X G. Deadlock control strategy in urban road network ［J］. *Journal of Highway in China*, 2010, **23**(6):96 － 102. （in Chinese）

［18］Yoshii T, Yonezawa Y, Kitamura R. Evaluation of an area metering control method using the macroscopic fundamental diagram ［C］//*Proceedings of the* 12*th World Conference on Transportation Research* (*WCTR*). Lisbon, Portugal, 2010:1 － 12.

［19］Keyvan-Ekbatani M, Kouvelas A, Papamichail I, et al. Exploiting the fundamental diagram of urban networks for feedback-based gating ［J］. *Transportation Research Part B*: *Methodological*, 2012, **46**(10):1393 － 1403. DOI: 10. 1016/j. trb. 2012. 06. 008.

［20］Wang F J, Wei W, Wang D H, et al. Identifying and monitoring the traffic state in urban road network based on macroscopic fundamental diagram ［C］//*Proceedings of Intelligent Transport Annual Meeting*. Hefei, China, 2012:35 － 39. （in Chinese）

［21］Li Y S, Xu J M, Shen L. A perimeter control strategy for oversaturated network preventing queue spillback ［J］. *Procedia—Social and Behavioral Sciences*, 2012, **43**:418 － 427. DOI:10. 1016/j. sbspro. 2012. 04. 115.

基于宏观基本图的路网边界信号控制策略

徐建闽　　鄢小文　　马莹莹　　荆彬彬

（华南理工大学土木与交通学院, 广州 510640）

摘要:为了解决过饱和区域的信号控制问题,基于宏观基本图理论研究过饱和区域的边界信号控制策略. 首先,通过 VISSIM 仿真软件构造特定区域路网的宏观基本图. 然后,根据宏观基本图确定该路网所能承载的最大累积车辆数. 基于路网可承载的最大累积车辆数建立区域边界交通信号控制策略,通过监控路网车流输入量、路网内总车辆数以及路网流出量,调整路网内边界交叉口的信号配时. 最后,针对虚拟路网建立了仿真模型,并设计 3 种流量需求方案对控制效果进行验证. 仿真结果表明,边界控制策略实施后路网的驶入驶出量大大提高,路网能够维持较大的通行量;同时,边界进口道的排队长度得到了合理控制,且路网的平均停车次数、平均延误等指标均得到了改善. 因此,基于宏观基本图的边界信号控制策略是有效可行的.

关键词:宏观基本图;边界控制;绿信比优化;微观仿真

中图分类号:U491